X-Ray Photoelectron Spectroscopy of Spinodal Decomposition in $Zn_{1-x}Co_xO$: Composition Dependence of Electronic Structure and Sputtering-Induced Co^0 Formation

Michael A. White,[1] Tracy C. Lovejoy,[2] Stefan T. Ochsenbein,[1] Marjorie A. Olmstead,[2] and Daniel R. Gamelin[1,*]
[1]*Department of Chemistry, University of Washington, Seattle, Washington 98195, USA*
[2]*Department of Physics, University of Washington, Seattle, Washington 98195, USA*
(Submitted – 29 October 2009)

Spinodal decomposition may contribute to the interesting magnetic properties of diluted magnetic oxides such as cobalt-doped ZnO ($Zn_{1-x}Co_xO$), but little is known experimentally about the electronic structures of the resulting high concentration regions or how they may behave under various experimental probes. Here, X-ray photoelectron spectroscopy (XPS) is used to examine wurtzite $Zn_{1-x}Co_xO$ crystallites ($0.0 \le x \le 1.0$) that model these high concentration regions. With increasing x, the valence band edge shifts to smaller binding energies and the cobalt 2p peaks shift to greater binding energies. Reduction of Co^{2+} to Co^0 by argon ion (Ar^+) sputtering was also found to become markedly more facile with increasing x, placing spinodally segregated $Zn_{1-x}Co_xO$ at greater risk of yielding false-positive Co^0 XPS signals than dilute $Zn_{1-x}Co_xO$ with the same average composition.

DOI: 10.1103/PhysRevLett.97.037203 PACS numbers: 75.50.Pp, 71.55._i, 75.30._m, 81.15.Gh

The magnetic properties of the diluted magnetic semiconductor (DMS) $Zn_{1-x}Co_xO$ and related oxides continue to be hotly debated.[1] Various synthetic techniques and post-synthetic treatments have generated materials that are nominally the same yet show strikingly different magnetism. In some instances strong correlations between ferromagnetism and the reversible introduction of charge carriers by Zn vapor diffusion[2] or electrical gating[3] have been observed. Heavily n-doped $Zn_{1-x}Co_xO$ of high structural quality shows no ferromagnetism, however.[4] Several experiments have implicated grain boundaries in the activation of such oxide ferromagnetism,[5-8] but the relevant grain-boundary defects and their associated bound charge carriers have been challenging to explore thoroughly, either experimentally or theoretically.

One leading hypothesis proposed to explain the curiously robust high-temperature ferromagnetism in widely studied DMSs such as $Zn_{1-x}Co_xO$ invokes the notion that spinodal decomposition enhances magnetic correlations by increasing local magnetic ion concentrations (x_{loc}).[9-12] Spinodal decomposition alone does not appear to generate ferromagnetism in $Zn_{1-x}Co_xO$,[13] but it may be a necessary-but-not-sufficient condition for high-T_C ferromagnetism, e.g., also requiring donor defects. Difficulties arise in the investigation of spinodal decomposition in $Zn_{1-x}Co_xO$ because of the similar local electronic and structural environments of Co^{2+} and Zn^{2+} in the wurtzite lattice. Nevertheless, electronic absorption and magnetic circular dichroism spectroscopies have differentiated spinodally segregated $Zn_{1-x}Co_xO$ (large x_{loc}) from dilute $Zn_{1-x}Co_xO$ (small x_{loc}) using shifts in ligand-field transition energies, among other properties.[13]

A second frequently proposed hypothesis is that the ferromagnetism of this entire class of materials, and of $Zn_{1-x}Co_xO$ in particular, arises from undetected cobalt metal or cobalt/zinc intermetallic precipitates embedded within the sample matrix, because in some cases such inclusions have been detected.[14,15] Experimentally verifying this hypothesis requires methods that reliably detect metal inclusions and can correlate the presence of such inclusions with ferromagnetism. A powerful technique widely applied for this purpose is X-ray photoelectron spectroscopy (XPS), because XPS is sensitive to changes in dopant charge state and to local electronic structure perturbations within a given charge state. Since XPS is a surface technique, it is usually used in conjunction with argon ion (Ar^+) sputtering, which removes surface carbon and can be used for depth profiling. XPS has recently provided key evidence supporting the hypothesis of metal inclusions as the common origin of $Zn_{1-x}Co_xO$ ferromagnetism.[4,16]

In this letter, we describe XPS experiments on a series of $Zn_{1-x}Co_xO$ crystallites with nominal Co^{2+} concentrations of x = 0.00, 0.05, 0.10, 0.40, 0.90, and 1.00, and with average grain diameters of ~10–20 nm. The crystallites were prepared as colloids and characterized structurally, optically, and magnetically as described in detail previously.[13] The data presented here demonstrate that XPS can indeed differentiate between the similar tetrahedral Co^{2+} ions of dilute (small x_{loc}) and concentrated (large x_{loc}) $Zn_{1-x}Co_xO$, both in the wurtzite lattice structure. Moreover, the results also show that Ar^+ sputtering of Co^{2+}-enriched $Zn_{1-x}Co_xO$ leads to formation of Co^0 with disproportionate ease, even under relatively mild sputtering conditions. These results demonstrate a relationship between two of the leading hypotheses for magnetic ordering of oxide DMSs: $Zn_{1-x}Co_xO$ samples with clustered Co^{2+} magnetic ions are far more likely to show Co^0 peaks in their XPS spectra than samples with uniformly distributed Co^{2+} ions, due to inadvertent Co^{2+} reduction during Ar^+ sputtering.

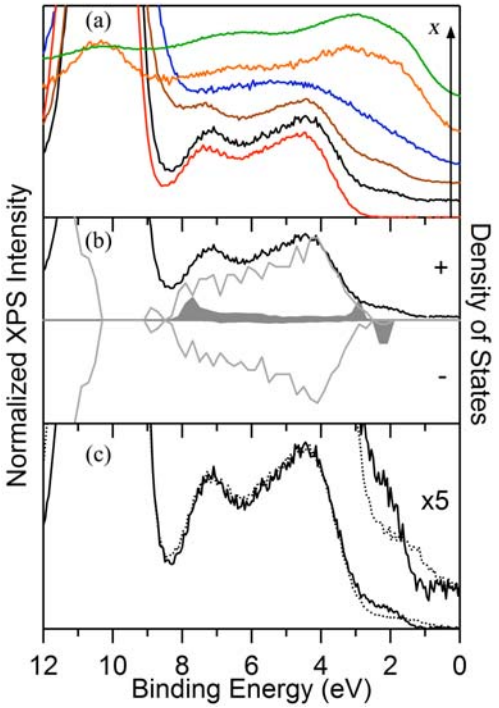

FIG. 1 (color online). XPS data for the valence band and Zn 3*d* region of $Zn_{1-x}Co_xO$ crystallites. (a) Data for x = 0.00 (red), 0.05 (black), 0.10 (brown), 0.40 (blue), 0.90 (orange), and 1.00 (green) samples, normalized to the O 2*p* peak maximum and offset for clarity. (b) Comparison of the valence band XPS spectrum for x = 0.05 (black) with the spin-resolved total density of states (grey) and Co^{2+} partial density of states (filled, x10) calculated by density functional theory for x = 0.006 (adapted from Ref. [22]). The increasing intensity above the top of the ZnO valence band with increasing x is due to occupied Co^{2+} 3*d* levels. (c) XPS spectrum for x = 0.05 (solid curve) and sum of the XPS spectra for x = 0.00 and x = 1.0 weighted to yield x ~ 0.05 (dotted line, x_{loc} ~ 1.0).

Samples for XPS measurements were prepared by depositing the colloidal crystallites onto transparent conductive fluorine-doped tin oxide (FTO) substrates, which were then inserted into a commercial XPS instrument (PHI VersaProbe) that uses monochromatic aluminum K_α excitation (1486 eV) and a hemispherical capacitor analyzer with an overall resolution of 0.6 eV (FWHM on Au 4f). Charge neutralization was carried out for all measurements using simultaneous electron and Ar^+ flood guns with accelerating voltages of 10 and 30 V, respectively. All spectra were aligned at the O 1*s* XPS binding energy[17] at 530.4 eV, which is known to arise from oxygen at a lattice site for ZnO.[14,16] A second oxygen peak observed at slightly higher energy (~532 eV) has been assigned as surface oxygen or hydroxide.[16,18] These O 2*s* peaks do not shift or broaden significantly with increasing x.

Figure 1(a) shows the valence band XPS spectra of several $Zn_{1-x}Co_xO$ samples of varying x. To the best of our knowledge, the XPS spectrum of wurtzite CoO (w-CoO, x = 1.00) has not been reported previously. At small x, Co^{2+} doping introduces new intensity ~1.5 eV shallower than the ZnO valence band, consistent with previous results.[19-21] For the x = 0.05 sample, Co^{2+} ionization occurs ~1.5 eV shallower than valence band ionization. This impurity intensity grows and shifts to lower binding energies as x is increased. Over the same series of samples, the Zn 3*d* XPS intensity (at ~10 eV) diminishes with increasing x before disappearing at x = 1.00. Figure 1(b) shows the XPS spectrum of the x = 0.05 sample (black line) plotted along with the spin-resolved total density of states (grey line) and cobalt partial density of states (filled, ×10) for $Zn_{1-x}Co_xO$ (x = 0.006), calculated by density functional theory.[22] The calculated binding energies were shifted to align with the experimental spectrum in the ZnO valence band region.

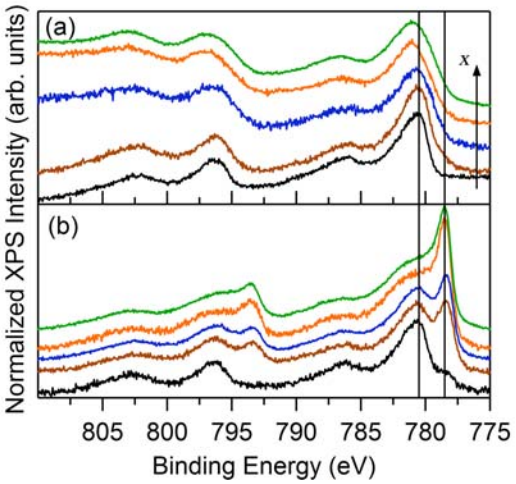

FIG. 2 (color online). (a) Normalized cobalt 2*p* XPS data for x = 0.05 (black), 0.10 (brown), 0.40 (blue), 0.90 (orange), and 1.00 (green) $Zn_{1-x}Co_xO$ crystallites collected without sputtering. The Co^{2+} $2p_{3/2}$ and $2p_{1/2}$ peaks shift to higher binding energies with increasing x. The lines at 778.5 and 780.7 eV are guides to the eye. The spectra are normalized to the Co^{2+} $2p_{3/2}$ intensity at 781 eV and offset for clarity. (b) Spectra of the same series of samples collected after sputtering, showing increasing Co^0 formation with increasing x.

The good overall agreement between experimental[4] and calculated results [Fig. 1(c)] confirms association of the new XPS intensity above the valence band maximum with the occupied Co^{2+} 3*d* levels. The optical transition involving promotion of these same Co^{2+} 3*d* electrons into the ZnO conduction band has been identified 1.5 eV below the ZnO band-to-band transition (3.4 eV),[23] in excellent agreement with the Co^{2+} XPS intensity that is ~ 1.5 eV above the ZnO valence band maximum [Fig. 1(b)]. Interestingly, optical data suggest that w-CoO is a charge-transfer insulator, with an optical band gap (2.3 eV) determined by the O^{2-}(2*p*)-to-Co^{2+}(3*d*) charge-transfer energy.[13] If this material were instead a Mott insulator, the band-gap excitation would have metal-to-metal charge-transfer character, but such transitions are estimated to occur at much higher energies (~5 - 6 eV),[24] than the experimental optical gap of w-CoO.[13] The data in Fig. 1(a) thus suggest the presence of localized Co^{2+} 3*d* levels at the top of an O 2*p*-derived valence band in w-

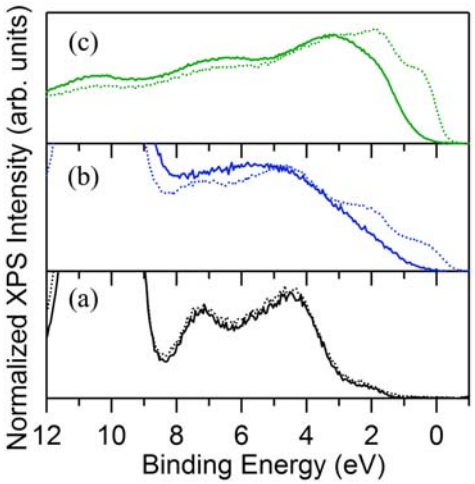

FIG. 3 (color online). Normalized valence band XPS spectra collected before (solid) and after (dotted) sputtering for x = (a) 0.05, (b) 0.40, and (c) 1.0 $Zn_{1-x}Co_xO$ crystallites.

CoO.

The data in Fig. 1(a) also suggest that XPS is a good experimental technique to distinguish between two samples with similar x but different x_{loc}: There is a clear shift in the onset of Co^{2+} 3*d* ionization by ~0.8 eV to lower binding energy from small x_{loc} to large x_{loc}. This distinction is illustrated in Fig. 1(c), which compares data for the x = 0.05 (x_{loc} ~ 0.05) sample with the simulated spectrum of an x ~ 0.05 (x_{loc} ~ 1.0) sample having the same integrated Co^{2+} 3*d* intensity, obtained from a linear combination of x = 1.0 and 0.0 spectra of Fig. 1(a). This comparison suggests that the valence band region of the XPS spectrum may be useful for identification of spinodal decomposition in $Zn_{1-x}Co_xO$.

Figure 2(a) shows Co 2*p* XPS spectra of the samples from Fig. 1. The spectra at small x agree well with previous results.[16,25] Cobalt $2p_{3/2}$ (780.5 eV) and $2p_{1/2}$ (796.2 eV) peaks are observed, as are shake-up satellites that indicate high-spin Co^{2+}.[16,25,26] Notably, there is no peak at 778.5 eV that would be indicative of Co^0.[16] Increasing x from 0.05 to 1.00 broadens the Co^{2+} peaks and shifts them by ~0.3 eV to higher binding energies. These changes are interpreted as greater inelastic scattering losses at large x, possibly due to short range magnetic coupling. The shift of the Co^{2+} 2*p* peak to higher binding energy (Fig. 2) and of the valence band to lower binding energy (Fig. 1) with increasing x are both manifestations of Co^{2+} electronic structural changes dependent on x and should therefore facilitate identification of spinodal segregation by XPS in other forms of $Zn_{1-x}Co_xO$ as well.

The data discussed above were all collected without Ar^+ sputtering, which is commonly used to remove carbon impurities and the top few nanometers of sample surface, either to increase XPS intensities or for depth profiling. We now describe the results obtained following relatively mild Ar^+ sputtering of the same samples discussed above. It has been shown[18] that sputtering cubic CoO at 5 kV for 2 hours can create Co^0, so the conditions used here

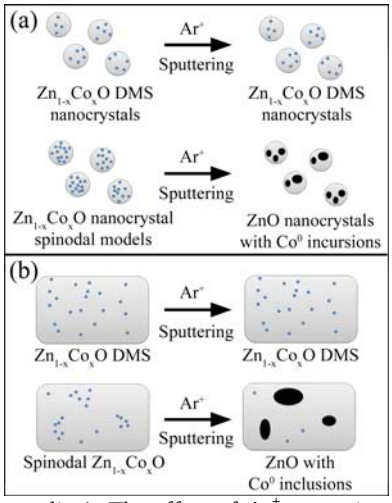

FIG. 4 (color online). The effect of Ar^+ sputtering on various $Zn_{1-x}Co_xO$ samples. (a) For the $Zn_{1-x}Co_xO$ crystallites studied here, sputtering causes little or no change in cobalt speciation when x is small, but Co^{2+} reduction becomes increasingly facile for increasing x, eventually leading to strong false-positive Co^0 XPS signals. (b) By analogy, $Zn_{1-x}Co_xO$ thin films or macrocrystals with spinodal Co^{2+} enrichments (large x_{loc}) may yield false-positive Co^0 XPS signals when sputtering is used to prepare their surfaces.

were deliberately gentle. Sputtering consisted of rastering 0.5 kV Ar^+ ions over a 2 mm by 2 mm area at an angle of 45 degrees for 30 seconds, repeated six times with two-minute wait periods between cycles. These conditions yielded etching sputtering rate of 1.6 nm/min (calibrated to SiO_2). The same sputtering parameters were applied for all samples.

The ZnO and small-x $Zn_{1-x}Co_xO$ samples showed little change with sputtering, the main effects being a loss of C 1*s* intensity, a loss of the higher-energy (surface) O 1*s* intensity, and an increase in all other intensities, consistent with previous observations.[16,18,25] At higher x, however, two new sharp peaks appeared at 778.5 and 793.5 eV that indicate sputtering-induced reduction of Co^{2+} to Co^0. The small Co^0 satellite peaks anticipated at ~4 eV higher binding energy[4] are presumably occluded by the Co^{2+} 2*p* peaks. Importantly, the relative intensities of these Co^0 peaks are *strongly* dependent upon the initial Co^{2+} concentration, with a larger fraction of Co^{2+} being reduced at higher x (Fig. 2[b]).

Sputtering generates new features in the valence band region as well, again strongly dependent upon x. Figure 3 shows data for three representative samples before (solid) and after (dashed) sputtering. Whereas the x = 0.05 sample (Fig. 3[a]) shows little change, the samples with greater x show new metallic states in the oxide band gap following sputtering. This new intensity is correlated with the Co^0 intensity at 778.5 eV from Fig. 2(b), and matches the density of states of cobalt metal.[17] Together, the introduction of metallic states at the Fermi level and growth of the Co^0 intensity at 778.5 eV indicate that sputtering-induced reduction of Co^{2+} to Co^0 is greatly facilitated at higher x.

These observations have bearing on the evaluation of spinodal decomposition, metallic impurity contamination, and other hypotheses for understanding the ferromagnetism of $Zn_{1-x}Co_xO$ and related DMSs. Although spinodal decomposition may enable stronger than expected magnetic correlations,[10-12] the results presented here indicate that it also greatly increases the propensity for Co^{2+} reduction by sputtering, which could lead to false-positive identification of Co^0 by XPS in samples that instead show spinodal decomposition.

Figure 4 summarizes these findings schematically. The formation of Co^0 by sputtering the spinodal models was much easier for larger x ($x > \sim 0.40$), even though the same crystallites without sputtering possessed exclusively Co^{2+} (Fig. 4[a]). Similar results are anticipated for other forms of $Zn_{1-x}Co_xO$ such as thin films (Fig. 4[b]): when x_{loc} is low, no sputtering-induced Co^0 formation is expected, but when x_{loc} is large, sputtering-induced Co^0 formation should become more facile. Indeed, 4 kV Ar^+ sputtering of $Zn_{1-x}Co_xO$ ($x = 0.30$) films for 5 minutes reportedly revealed similar new Co^0 XPS features,[16] and the data here strongly support the interpretation of these features as artifacts derived from sputter reduction of Co^{2+}.

In summary, XPS spectra of $Zn_{1-x}Co_xO$ ($0.0 \leq x \leq 1.0$) models of spinodal enrichments in $Zn_{1-x}Co_xO$ show modest shifts in the Co 2*p* and valence band ionization energy regions with increasing x that can be related to changes in Co^{2+} electronic structure within the ordered magnetic lattice with large x_{loc}, and that should assist identification of spinodal decomposition in other forms of the same material. The data also reveal an important link between x in wurtzite $Zn_{1-x}Co_xO$ and the observation of Co^0 by XPS: increasing x strongly facilitates sputtering-induced Co^0 formation, even under mild sputtering conditions. This relationship could potentially lead to false identification of metallic Co^0 inclusions in samples that actually possess spinodal enrichments of Co^{2+} (large x_{loc}). Overall, these data provide new information about the electronic structures of highly enriched spinodal phases in $Zn_{1-x}Co_xO$, and demonstrate the characterization of such phases by XPS with findings that have bearing on evaluation of the roles of spinodal decomposition and Co^0 inclusions in the high-temperature ferromagnetism of this and other oxide DMSs.

This work was funded by NSF grants (CRC-0628252 (DRG) and DMR-0605601 (MAO, TCL). MAW was supported through te UW-CNT as an NSF/NCI IGERT trainee (DGE-0504573). The XPS instrumentation was funded by the Micron Foundation.

*Electronic address: Gamelin@chem.washington.edu.

[1] S. J. Pearton, D. P. Norton, M. P. Ivill, A. F. Hebard, J. M. Zavada, W. M. Chen, and I. A. Buyanova, IEEE Trans. Electron Devices **54**, 1040 (2007).
[2] K. R. Kittilstved, D. A. Schwartz, A. C. Tuan, S. M. Heald, S. A. Chambers, and D. R. Gamelin, Phys. Rev. Lett. **97**, 037203 (2006).
[3] H.-J. Lee, E. Helgren, and F. Hellman, Appl. Phys. Lett **94**, 212106 (2009).
[4] T. C. Kaspar, T. Droubay, S. M. Heald, P. Nachimuthu, C. M. Wang, V. Shutthanandan, C. A. Johnson, D. R. Gamelin, and S. A. Chambers, New Journal of Physics **10**, 055010 (2008).
[5] P. I. Archer and D. R. Gamelin, J. Appl. Phys. **99**, 08M107 (2006).
[6] T. C. Kaspar, T. Droubay, V. Shutthanandan, S. M. Heald, C. M. Wang, D. E. McCready, S. Thevuthasan, J. D. Bryan, D. R. Gamelin, A. J. Kellock, M. F. Toney, X. Hong, C. H. Ahn, and S. A. Chambers, Phys. Rev. B **73**, 155327 (2006).
[7] T. C. Kaspar, S. M. Heald, C. M. Wang, J. D. Bryan, T. Droubay, V. Shutthanandan, S. Thevuthasan, D. E. McCready, A. J. Kellock, D. R. Gamelin, and S. A. Chambers, Phys. Rev. Lett. **95**, 217203 (2005).
[8] P. V. Radovanovic and D. R. Gamelin, Phys. Rev. Lett. **91**, 157202 (2003).
[9] T. Dietl, T. Andrearczyk, A. Lipinska, M. Kiecana, M. Tay, and Y. Wu, Phys. Rev. B **76**, 155312 (2007).
[10] T. Fukushima, K. Sato, H. Katayama-Yoshida, and P. H. Dederichs, Jap. J. Appl. Phys. **45**, L416 (2006).
[11] K. Sato, T. Fukushima, and H. Katayama-Yoshida, Jpn. J. Appl. Phys. **46**, L682 (2007).
[12] K. Sato, H. Katayama-Yoshida, and P. H. Dederichs, Jap. J. Appl. Phys. **44**, L948 (2005).
[13] M. A. White, S. T. Ochsenbein, and D. R. Gamelin, Chem. Mater. **20**, 7107 (2008).
[14] T. C. Kaspar, T. Droubay, S. M. Heald, M. H. Engelhard, P. Nachimuthu, and S. A. Chambers, Phys. Rev. B **77**, 201303(R) (2008).
[15] J. H. Park, M. G. Kim, H. M. Jang, S. Ryu, and Y. M. Kim, Appl. Phys. Lett **84**, 1338 (2004).
[16] M. Ivill, S. J. Pearton, S. Rawal, L. Leu, P. Sadik, R. Das, A. F. Hebard, M. Chisholm, J. D. Budai, and D. P. Norton, New Journal of Physics **10**, 065002 (2008).
[17] For more experimental details and XPS data please see EPAPS Document No XXX. For more information on EPAPS please see http://www.aip.org/pubservs/epaps.html.
[18] T. Choudhury, S. O. Saied, J. L. Sullivan, and A. M. Abbot, J. Phys. D: Appl. Phys. **22**, 1185 (1989).
[19] M. Kobayashi, Y. Ishida, J. l. Hwang, T. Mizokawa, A. Fujimori, K. Mamiya, K. Okamoto, Y. Takeda, T. Okane, Y. Saitoh, Y. Muramatsu, A. Tanaka, H. Saeki, H. Tabata, and T. Kawai, Phys. Rev. B **72** (2005).
[20] S. C. Wi, J. S. Kang, J. H. Kim, S. B. Cho, B. J. Kim, S. Yoon, B. J. Suh, S. W. Han, K. H. Kim, K. J. Kim, B. S. Kim, H. J. Song, H. J. Shin, J. H. Shim, and B. I. Min, Appl. Phys. Lett. **84**, 4233 (2004).
[21] S. C. Wi, J.-S. Kang, J. H. Kim, S. S. Lee, S.-B. Cho, B. J. Kim, S. Yoon, B. J. Suh, S. W. Han, K. H. Kim, K. J. Kim, B. S. Kim, H. J. Song, H. J. Shin, J. H. Shim, and B. I. Min, Phys. Stat. Sol. (b) **241**, 1529 (2004).
[22] E. Badaeva, Y. Feng, D. R. Gamelin, and X. Li, New Journal of Physics **10**, 055013 (2008).
[23] W. K. Liu, G. M. Salley, and D. R. Gamelin, J. Phys. Chem. B **109**, 14486 (2005).
[24] J. van Elp, J. L. Wieland, H. Eskes, P. Kuiper, G. A. Sawatzky, F. M. F. de Groot, and T. S. Turner, Phys. Rev. B **44**, 6909 (1991).
[25] A. C. Tuan, J. D. Bryan, A. B. Pakhomov, V. Shutthanandan, S. Thevuthasan, D. E. McCready, D. Gaspar, M. H. Engelhard, J. W. Rogers Jr., K. Krishnan, D. R. Gamelin, and S. A. Chambers, Phys. Rev. B **70**, 054424 (2004).
[26] D. C. Frost, C. A. McDowell, and I. S. Woolsey, Molecular Physics **27**, 1473 (1974).

EPAPS Figures:

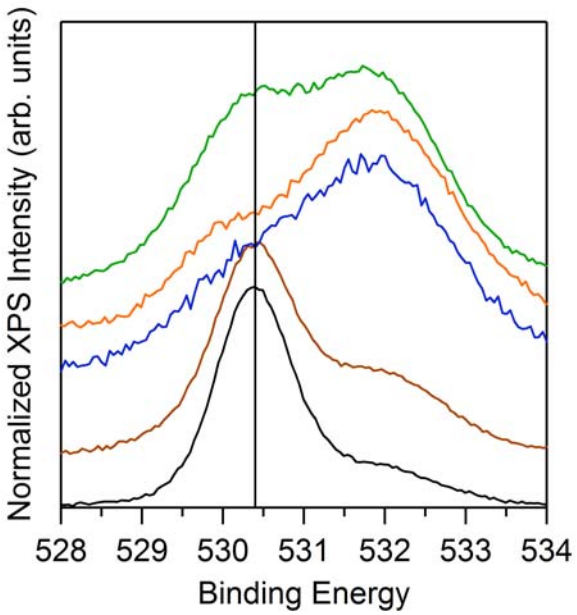

EPAPS Figure 1: O 1s XPS spectra for x = 0.00, x = 0.05, x = 0.10, x = 0.40, x = 0.90, and x = 1.00. The spectra are fit with two Gaussians with equal widths, and the binding energy is shifted so the lower energy Gaussian is centered at 530.4 eV.

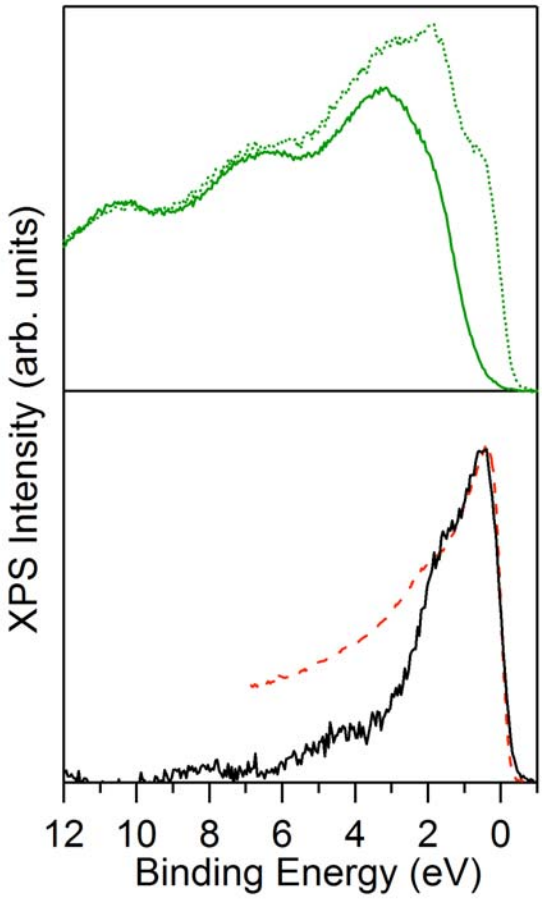

EPAPS Figure 2: (a) Normalized w-CoO before (solid) line and after (dotted) sputtering. The data from Figure 3 is rescaled for the best fit at higher binding energy. (b) Difference between (solid) before and after sputtering and (dashed) measured Co^0 XPS intensity. [Adapted from L. E. Klebanoff, D. G. Van Campen, and R. J. Pouliot, Phys. Rev. B **49**, 2047 (1994).]